Nuclear Instruments and Methods in Physics Research B 539 (2023) 102–107

Contents lists available at ScienceDirect

Nuclear Inst. and Methods in Physics Research, B

journal homepage: www.elsevier.com/locate/nimb

In-gas-jet laser spectroscopy with S^3-LEB

Anjali Ajayakumar [a,*], Jekabs Romans [d], Martial Authier [b], Yazeed Balasmeh [c], Alexandre Brizard [a], Frederic Boumard [c], Lucia Caceres [a], Jean-Francois Cam [c], Arno Claessens [d], Samuel Damoy [a], Pierre Delahaye [a], Philippe Desrues [c], Wenling Dong [e], Antoine Drouart [b], Patricia Duchesne [e], Rafael Ferrer [d], Xavier Fléchard [c], Serge Franchoo [e], Patrice Gangnant [a], Sarina Geldhof [a], Ruben P. de Groote [d], Fedor Ivandikov [d], Nathalie Lecesne [a], Renan Leroy [a], Julien Lory [c], Franck Lutton [a], Vladimir Manea [e], Yvan Merrer [c], Iain Moore [f], Alejandro Ortiz-Cortes [a], Benoit Osmond [a], Julien Piot [a], Olivier Pochon [e], Sebastian Raeder [h,i], Antoine de Roubin [d], Hervé Savajols [a], Dominik Studer [g], Emil Traykov [j], Juha Uusitalo [f], Christophe Vandamme [c], Paul Van den Bergh [d], Piet Van Duppen [d], Klaus Wendt [g]

[a] GANIL, CEA/DRF-CNRS/IN2P3, B.P. 55027, 14076 Caen, France
[b] IRFU, CEA, Université Paris-Saclay, F-91191 Gif sur Yvette, France
[c] Université de Caen Normandie, ENSICAEN, CNRS/IN2P3, LPC Caen UMR6534, F-14000 Caen, France
[d] KU Leuven, Instituut voor Kern- en Stralingsfysica, B-3001 Leuven, Belgium
[e] Université Paris-Saclay, CNRS/IN2P3, IJCLab, 91405, Orsay, France
[f] Department of Physics, University of Jyväskylä, PO Box 35 (YFL), Jyväskylä FI-40014, Finland
[g] Institut für Physik, Johannes Gutenberg-Universität Mainz, 55128 Mainz, Germany
[h] GSI Helmholtzzentrum für Schwerionenforschung GmbH, Planckstraße 1, Darmstadt, 64291, Germany
[i] Helmholtz Institute Mainz, Staudingerweg 18, 55128 Mainz, Germany
[j] IPHC, Université de Strasbourg, CNRS, F-67037 Strasbourg, France

ARTICLE INFO

Keywords:
Atomic spectroscopy
Resonance-ionization laser spectroscopy
Gas cell
Gas-jet

ABSTRACT

The Super Separator Spectrometer-Low Energy Branch (S^3-LEB) is a low-energy radioactive ion beam experiment under commissioning as part of the GANIL-SPIRAL2 facility. It will be used for the production and study of exotic nuclei by in-gas laser ionization and spectroscopy (IGLIS), decay spectroscopy, and mass spectrometry. We report recent results from the off-line commissioning of S^3-LEB, including first laser spectroscopy measurements in both the gas cell and the supersonic gas jet, the determination of the transport efficiency of laser ions from the gas cell through the RFQ chain, and time-of-flight measurements with the multi-reflection time-of-flight mass spectrometer PILGRIM. The measurements were performed using erbium, introduced by evaporation from a heated filament in the gas environment. The reported laser spectroscopy results include a characterization of the pressure broadening in the gas cell, proof-of-principle isotope shift measurements, and hyperfine-structure measurements.

1. Introduction

The SPIRAL2 facility of the Grand Accélérateur National d'Ions Lourds (GANIL) is a radioactive ion beam (RIB) laboratory enabling the study of rare isotopes. Its linear accelerator is designed to deliver heavy-ion beams with some of the highest intensities ever produced [1,2]. To exploit them, the Super Separator Spectrometer (S^3), a high-resolution recoil separator, will use these high-intensity beams to produce exotic nuclei via fusion–evaporation reactions and is designed to separate the reaction products from the intense primary beams [3,4]. The facility will extend the capabilities to study exotic nuclei with low production rates and short lifetimes. One of the setups to be installed at the focal plane of S^3 is the Super Separator Spectrometer-Low Energy Branch (S^3-LEB), which is aimed at the study of neutron deficient and heavy nuclei via a combination of low-energy techniques, after stopping them in a thermalization and neutralization gas cell [5–8].

The key feature of the setup is the possibility to apply the in-gas laser ionization and spectroscopy (IGLIS) technique, which allows the study of the exotic nuclei by laser spectroscopy at the proximity of

* Corresponding author.
E-mail address: anjali.ajayakumar@ganil.fr (A. Ajayakumar).

https://doi.org/10.1016/j.nimb.2023.03.020
Received 23 February 2023; Accepted 15 March 2023
Available online 3 April 2023
0168-583X/© 2023 Elsevier B.V. All rights reserved.

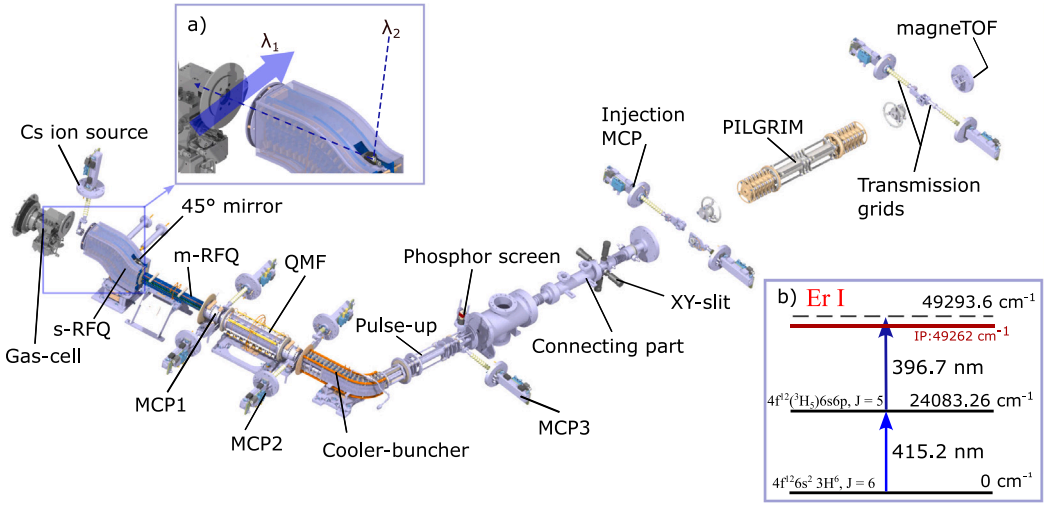

Fig. 1. Layout of the S^3-LEB setup: Inset (*a*) shows a zoom of the gas-jet region of the setup with λ_1 and λ_2 indicating the first-step and second-step laser paths and (*b*) shows the applied laser scheme for resonance ionization of the Er atoms. See text for details.

their stopping point. Furthermore, as shown in [6,9], a high-resolution tunable laser system will be used to selectively ionize and probe the radioactive atoms in the low-density and low-temperature environment of the hypersonic gas jet emerging from the cell. The gas-jet laser spectroscopy technique benefits from the reduced pressure and Doppler broadening of the spectral lines, as compared to traditional gas-cell or hot cavity laser spectroscopic setups [10–12].

In this manner, S^3-LEB will offer improved spectral resolution as well as high ionization efficiency, enabling measurements of the ground-state and isomeric-state isotope shifts and hyperfine structure as previously demonstrated at the Leuven Isotope Separator On Line (LISOL) facility [13]. The coupling of a multi-reflection time of flight mass spectrometer (MR-TOF-MS) called Piège à Ions Linéaire du GANIL pour la Résolution des Isobares et la mesure de Masse (PILGRIM) [7] and a decay station called Spectroscopy Electron Alpha in Silicon bOx couNter (SEASON) [14] at the S^3-LEB setup offers opportunities for further mass measurements and decay-spectroscopy studies of high purity RIBs with the suppression of isobaric contamination.

Recently, the setup of the entire S^3-LEB, including the gas cell, radiofrequency quadrupole (RFQ) ion guides, ion cooler and buncher, and MR-TOF MS was completed and commissioned using laser ions produced in a gas environment. In this article, we present an update on the characterization studies of the setup, including the first off-line laser spectroscopy measurements.

2. S^3-LEB setup

The S^3-LEB setup is currently being tested off-line at Laboratoire de Physique Corpusculaire (LPC), Caen. The complete layout of the installation in its current configuration is shown in Fig. 1. For the first in-gas cell/jet measurements, all the components from the gas cell to the MR-TOF-MS have been installed, connected and aligned. SEASON is not included in the current system.

In on-line conditions at SPIRAL2, the S^3 ion beam will enter the gas cell through a titanium or Mylar entrance window of a few micrometers thickness. The cell will be filled with ultrapure argon buffer gas under constant flow, reaching a pressure of 200–500 mbar for efficient stopping of the atoms. The geometry of the gas cell has been designed for maximal flow rate thus minimal extraction time of the atoms [6]. The window will separate the vacuum region of S^3 from the higher-pressure region of the gas cell. The radioactive ions will thermalize and neutralize in the buffer gas. For off-line studies, the gas cell was operated as it will be in on-line conditions, but the entrance window was replaced by a blind flange. Two tantalum filaments were installed in the gas cell, on which stable isotopes of the element under study were deposited in solution form, allowing their evaporation as neutral atoms directly into the gas environment through resistive heating.

The atoms are flushed out of the gas cell through a convergent–divergent (de-Laval) nozzle installed at the exit, which creates a homogeneous argon gas jet [15]. Two ion-collector electrodes installed before the exit nozzle of the gas cell enable suppression of non-neutralized species or surface ions resulting from the heated tantalum filament. During operation, argon is injected into the gas cell through a heated getter gas purifier model Saes PB4-MT3-R-2. The gas flow is pumped out of the gas cell chamber by an Edwards pump model GXS450/4200. The background pressure is matched to the gas-jet pressure, imposed by the Mach number of the nozzle to obtain a homogeneous and collimated gas jet [12,16], using a motorized gate valve of variable opening between the chamber and the GXS pump.

Multiple lasers are used for selectively ionizing the atoms of interest, either inside the gas cell or in the gas jet. The laser system installed for the off-line measurements consists of two titanium sapphire (Ti:sapphire) lasers with a repetition rate of 10 kHz which are part of the system reported in [9,17–20]. Following ionization, the resulting ions are extracted through an S-shaped RFQ (S-RFQ) and mini-RFQ (m-RFQ) from the residual pressure of the gas-cell chamber into a high-vacuum ion-transport system. Following the m-RFQ, a quadrupole mass filter (QMF) is installed as a pre-separator according to the ions' mass-to-charge ratio, A/Q. The QMF can be operated in high-transmission mode (without mass selection) as well as in mass-filtering mode. The voltages used in this work for the S-RFQ, m-RFQ, and QMF are adapted from those reported in [8]. The ion beam from the QMF is guided to the RFQ cooler-buncher where the ions are buffer-gas cooled in helium at a pressure on the order of 1×10^{-2} mbar, obtained by a continuous flow of 90–120 mL/min. Ions are continuously accumulated and bunched with a repetition rate of 20 Hz. Following extraction from the buncher by switching the voltages of the last electrodes to an extraction gradient, the ions are re-accelerated to 3 keV mean kinetic energy by a switched pulse-up electrode and injected into the PILGRIM MR-TOF-MS for time-of-flight separation and mass measurement. For detection of the ion signals, micro-channel plate (MCP) detectors are installed behind the m-RFQ (MCP1), QMF (MCP2), and pulse-up electrode (MCP3) and a MagneTOF Mini detector is installed after PILGRIM. MCP1 and MCP2 have 10% transmission grids installed in front of them to attenuate intense beams and can also be used to measure ion current. MCP3 has two 10% transmission grids and a phosphorous screen allowing to observe the spatial beam profile using a camera. The second transmission grid can be biased and

used as a retarder to determine the energy spread of the beam. For laser-spectroscopy measurements, the MCP counts are digitized with respect to time with a resolution of 4 ns/bin using a time-to-digital converter (TDC) developed by KU Leuven and synchronized to the 20 Hz cycle of the buncher. For mass measurements using PILGRIM, the Fast Acquisition System for Nuclear Research (FASTER) developed by LPC Caen [21] is used.

3. Off-line measurements

For the initial off-line measurements of S^3-LEB, stable Er was used as a test case. The laser ionization of the Er isotopes was performed with the two-step laser scheme, developed and reported in [22], and is indicated in Fig. 1. The Er atoms were promoted from the ground state $4f^{12}6s^2\ ^3H_6$, J = 6 to the first excited state (FES) $4f^{12}(^3H)6s6p$, J = 5 by a laser tuned to 415.2 nm vacuum wavelength and then ionized via an autoionizing state above the ionization potential (IP), $4f^{12}(^3H)5p^6 6s_{1/2}$ J = 13/2, by a laser tuned to 396.6 nm. For the first excitation step in gas-cell ionization, we used a frequency-doubled, dual-etalon Ti:sapphire laser cavity, with an average fundamental linewidth of 1.8 GHz FWHM. For the same step in gas-jet ionization, we used a frequency-doubled, injection-locked Ti:sapphire laser seeded by an external-cavity diode laser [19]. A TEM Messtechnik Laselock lock-in amplifier was used to stabilize the injection-locked cavity to the frequency of the seeding diode, resulting in an average fundamental linewidth of about 35 MHz. For the ionization step in both configurations, we used a frequency-doubled, single-etalon Ti:sapphire laser of average fundamental linewidth ≤ 5 GHz FWHM.

The laser systems were installed and set up similarly to the work performed in [9]. For laser-spectroscopy scans, the dual-etalon laser was controlled using stepper motors. The thick etalon was tuned to the required angle based on a proportional controller to achieve the desired wavelength, while the thin etalon was adjusted to guarantee constant linewidth, following a calibration curve [18]. The wavelength of the injection-locked laser was set by controlling the grating angle of the seeding diode, while the Laselock adjusted the cavity length accordingly.

3.1. Production and transport

To produce Er ions, a 30 μL Er_2O_3 in HNO_3 solution was deposited on each of the two tantalum filaments installed in the gas cell. One of the filaments was resistively heated by ≈ 13 A (4 V) current. At the exit aperture of the gas cell, a de-Laval nozzle of Mach number $M = 8.11(12)$ was installed to create a hypersonic gas jet [15]. The distance between the nozzle and the first entrance electrode of the S-RFQ was kept about 5–6 cm. For gas-cell ionization, the first-step and second-step lasers were sent transverse and counter-propagating to the atomic beam, respectively.

The combined efficiency of the S-RFQ and m-RFQ had already been measured to be close to 100% using an alkali source placed approximately at the jet position, although having a much larger emittance than the laser ions produced in the jet [8]. After passing through the S-RFQ and m-RFQ, the Er ions were sent through the QMF in transmission mode to obtain close to 100% transmission. A minimum ion-collector voltage of −40 V in the gas cell was required to completely suppress the surface ions produced by the filament. The filament current was adjusted to obtain around 6300 cps at MCP 2 after the QMF. A mass scan was then performed with the QMF in filtering mode, by scanning the RF and DC voltages such that, for the requisite masses, a Mathieu parameters $a = 0.225$, and $q = 0.706$ would be obtained, with an RF frequency of 500 kHz (knowing the QMF field radius of 10 mm). Fig. 2 shows the resulting mass spectrum, where only ions in the Er mass range can be seen along with a small side peak which corresponds to adducts of Er with water molecules, formed after laser ionization. In the filtering mode, the QMF transmission was 60%, with respect to the maximum number of ion counts detected in the non-filtering mode. Individual Er isotopes could not be resolved after the QMF, which however is capable of selecting a range of about 10 mass units without a major loss in efficiency. For the rest of the tests, the QMF was kept in transmission mode.

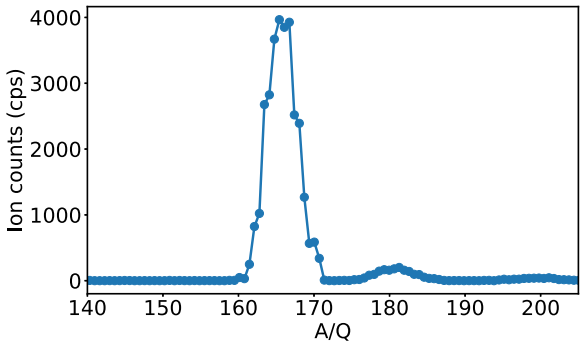

Fig. 2. QMF mass scan of gas-cell ions obtained by scanning the RF and DC voltage, with the gas cell ion-collector voltage ON.

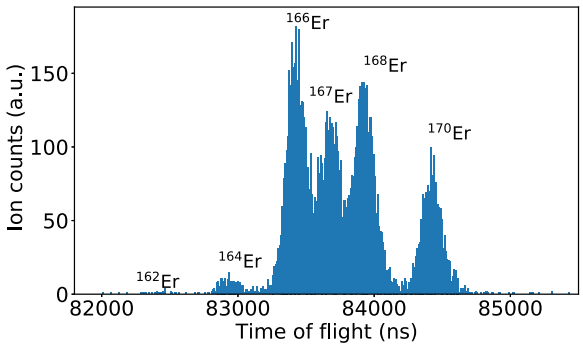

Fig. 3. Time-of-flight spectra of laser-produced Er ions in a shoot-through mode of the MR-TOF MS with the ion-flight path length of ≈ 4.2 m from the buncher extraction.

The continuous beam from the QMF was then sent to the cooler-buncher. A detailed study of the bunching parameters was performed to understand the optimum spatial and energy distribution of the bunches for injection into PILGRIM. These results will be reported in future publications. The preliminary buncher transmission efficiency in the bunching configuration is 40(10)%. The relatively low value could be due to an observed misalignment of the buncher, which will be investigated in more detail in the future. The spatial profile of the 20 Hz cycle ion bunch at a He flow rate of 110 mL/min was measured to be 1.5(4) mm on both the vertical and horizontal axes as seen from the phosphor screen of MCP3. The energy distribution of the ion bunch was also measured at a 3 keV mean kinetic energy resulting in a FWHM = 13(1) eV after the pulse-up electrode. The transmission from the buncher (in bunching configuration) to the end of PILGRIM without trapping was found to be 50(20)%. Fig. 3 shows the obtained PILGRIM shooting-through time-of-flight (TOF) spectrum of all the stable Er isotopes, with first-step and second step lasers kept at a fixed frequency, agreeing roughly with the natural isotopic abundance. The obtained TOF width for ^{170}Er without trapping was with mean TOF ≈ 84.4 μs from the buncher extraction to the end of PILGRIM and FWHM of 179(8) ns, with optimization still in progress. The preliminary resolving power obtained is $R \approx 80,000$ for 1000 revolutions which can be improved to the order of $R \approx 10^5$ as seen from the tests with alkali elements [7,23,24].

3.2. In-gas-cell laser spectroscopy

For the laser spectroscopy measurements, the saturation curve for the FES transition was measured before the gas cell chamber and the

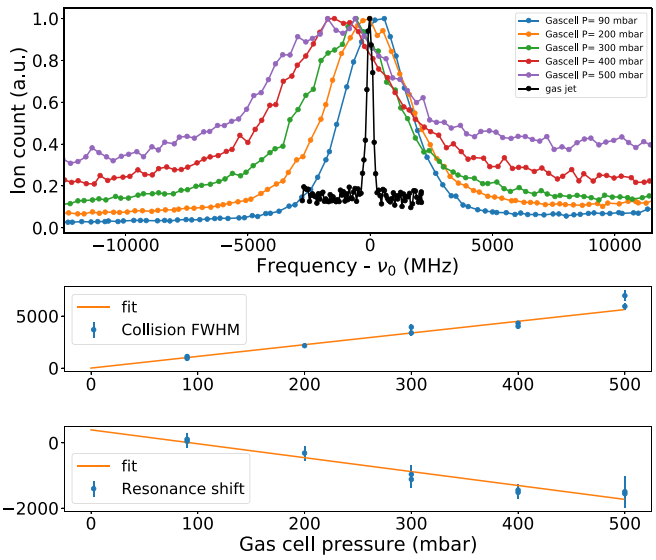

Fig. 4. (Top) Resonance ionization spectroscopy of Er in the gas cell for different gas pressures (color) compared to the gas-jet spectroscopy of ^{170}Er (black) for the FES transition relative to ν_0 = 721,995,050 MHz. (Middle and bottom) Collision FWHM and centroid shift were determined for the spectra as a function of pressure. A linear fit is applied to the data to extract the pressure broadening and pressure shift coefficients discussed in the text.

laser power was kept at 0.1 mW, well below the saturation power where no more power broadening of the spectrum was observed. The second-step laser power was kept at 50 mW. In the gas cell, the collisions of the atoms with buffer gas cause collisional broadening of the spectrum [25,26]. This broadening can be several GHz wide, which limits precise measurements of atomic isotope shifts and hyperfine constants. The ionization efficiency can also be strongly influenced by the gas effects such as the collisional de-excitation [27]. In-gas-cell resonant laser ionization of Er atoms was performed and characterized for different gas cell pressures. The broadening of the Er excitation spectral lines was studied by scanning the laser frequency over the FES transition resonance peak. Fig. 4 (top panel) shows the gas cell FES transition spectra as a function of argon gas cell pressures from 90–500 mbar, compared to a single resonance measured for ^{170}Er in the gas jet. The laser frequency measurements for the in-jet spectroscopy were performed with a HighFinesse WS7 wavemeter with an accuracy of 30 MHz (fundamental), while the gas cell measurements were performed with a WS6 version, having an absolute accuracy of 600 MHz. It can be seen that the resonances broaden and experience a centroid shift to lower frequencies with an increase in the gas cell pressure [12]. The reference transition frequency corresponds to the in-jet resonance of ^{170}Er which is ν_{01} = 721,995,054(60) MHz. The value is within the wavemeter accuracy of the transition frequency deduced from the atomic beam unit (ABU) measurements (ν_{01} = 721,995,048(60) MHz) [9]. The natural spectral linewidth depends on the transition probability (9.6×10^7 s^{-1}) and can be calculated to be 15.3 MHz which is negligible compared to the collisional broadening effect [28]. The first-step laser linewidth for gas-cell ionization was an average of 1.8 GHz FWHM. The Doppler FWHM for the FES transition at an estimated gas cell temperature of T = 353(16) K was calculated to be 0.75(2) GHz [12].

Spectra for the different gas cell pressures were fitted with a Voigt profile, using the Statistical analysis toolbox for laser spectroscopy (SATLAS) package [29]. For individual gas cell pressures, the Gaussian FWHM (calculated from the Doppler FWHM and the laser FWHM linewidth) were fixed to 2654(226) MHz in the fitting procedure to obtain the resonance center and the Lorentzian FWHM, the latter being entirely due to the collisional broadening and the natural transition linewidth. A linear least-squares fit was applied to the resulting collisional FWHM and resonance shift data as a function of different gas cell pressures from which the collisional broadening coefficient (Γ_{coll}) and the shift coefficient (Γ_{sh}) were deduced to be 11(1) MHz/mbar and -4(1) MHz/mbar, respectively. The data (blue) and the resulting fit (orange) are shown in the lower two panels of Fig. 4. The centroid shift from the fit line extrapolates to 398(143) MHz for zero gas cell pressure. Since argon is used as the buffer gas, the shift coefficient has a negative sign, i.e, the centroid is red-shifted [25]. For the measurements, ion counts were detected after the QMF and therefore the individual isotopes could not be distinguished. However, this should not affect the measured values as the isotope shift between the different isotopes is in the order of 100 MHz, whereas the broadening of the gas-cell spectra is several GHz. The spectral FWHM for a gas cell pressure of 300 mbar was measured to be on average 4.5(2) GHz.

3.3. In-gas-jet laser spectroscopy

To perform resonance ionization spectroscopy in the gas jet, the gas-jet chamber was pumped to a pressure of 1.25×10^{-1} mbar for a gas cell pressure of 300 mbar. This was to match the background pressure with the gas jet pressure in order to obtain a homogeneous jet for laser spectroscopy studies. Two laser configurations were used and characterized, with the first-step laser aligned either counter-propagating or transverse to the gas jet, while the second-step laser was transverse and counter-propagating, respectively. For the transverse laser path in the jet, a laser beam sheet of width 2 mm and length 50 mm was prepared using a combination of two cylindrical lenses (focal length, f_1 = -20 mm and f_2 = 250 mm). A saturation curve for the FES transition with the injection-locked laser was measured. For the transverse configuration, the first-step laser power was kept below 1 mW (measured before the laser sheet) to minimize the power broadening. The second-step laser power was kept around 170–200 mW. The second-step laser was reoptimized to obtain higher count rates for gas-jet spectroscopy measurements and hence the higher power compared to the gas-cell spectroscopy measurements. Measurements performed in both laser configurations gave a spectral resolution of less than 300 MHz FWHM. Fig. 4 (top panel) shows a comparison of the gas cell (color) and gas jet spectra (black). The values were scaled to 1 for comparison. The obtained gas jet ion counts were more than triple compared to the gas cell ion counts for the same second-step laser powers. More systematic studies of the jet ionization efficiency will be performed in the future. Resonance-ionization laser spectroscopy of stable Er isotopes (except ^{162}Er) in the gas jet using first excitation was performed. The representative spectra are shown in Fig. 5. The weighted average of the spectral FWHM obtained is 281(5) MHz. The isotope shifts (IS) for $^{170-164}$Er with ^{170}Er as the reference isotope as well as the hyperfine A and B constants of the odd isotope ^{167}Er were determined (see Table 1). To perform the measurements, the laser frequency was scanned over the resonances for the individual isotopes, and the MagneTOF counts after PILGRIM were recorded using the Leuven TDC. The bunched ions were trapped for three revolutions in PILGRIM to have an increased time-of-flight allowing to separate the Er isotopes. The spectra were fitted with a Voigt profile, using the SATLAS package as shown in Fig. 5, fixing the relative intensities of the hyperfine components by the corresponding Racah coefficients for ^{167}Er. The hyperfine A and B constants were determined in two ways, firstly by keeping the A and B parameters for the $4f^{12}\ 6s^2\ ^3H_6$ ground state free and secondly, by fixing them to literature values, leaving free only the parameters of the excited state, for the fit. The results of both methods of fitting are in agreement with the literature [9,30–32]. The total uncertainties were estimated following the approach detailed in [9], considering the statistical uncertainties, the scattering of the values from the individual scans, and the systematic errors of the wavemeter.

For estimating the Mach number of the jet, defined as the ratio of stream velocity (u) to the local speed of sound (a), calculations

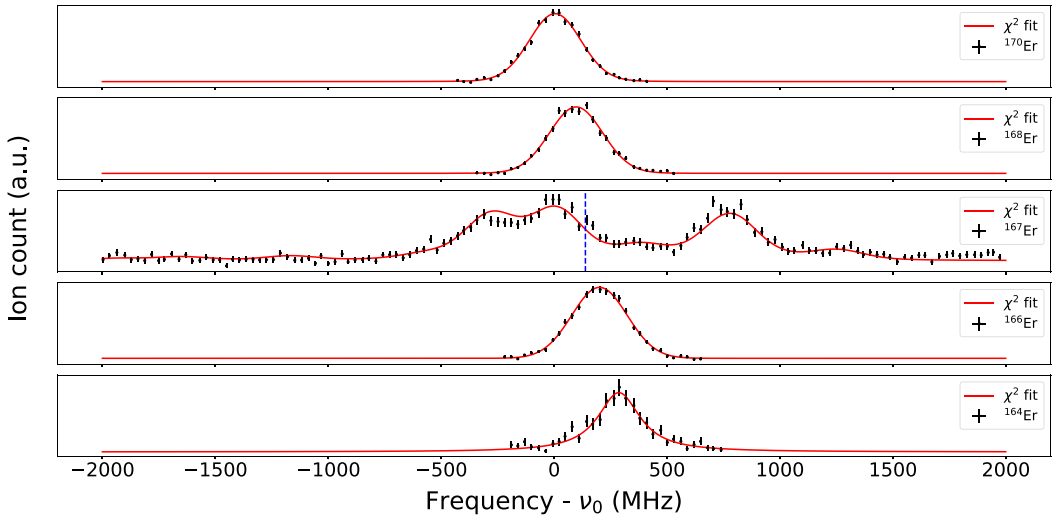

Fig. 5. Laser spectroscopy of stable Er isotopes in the gas jet using the first excitation step relative to ν_0 = 721,995,050 MHz. The first-step laser was sent in a transverse geometry and the second-step laser in a counter-propagating direction to the Er atomic beam. The measured data points (black) are normalized by the laser powers of both steps and the fit is shown in red. The weighted centroid for ^{167}Er is marked as the blue dashed line.

Table 1
IS values $\Delta\nu^{A',170} = \nu^{A'} - \nu^{170}$ of stable $^{168-164}$Er isotopes with respect to ^{170}Er and hyperfine A and B constants, for the $4f^{12}6s^2\ ^3H_6$ and $4f^{12}(^3H)6s6p\ J = 5$ atomic states of ^{167}Er deduced from the gas jet measurements, are shown and compared with the literature values reported in [9,31,32]. Fit values with A and B for the ground state kept free and fixed are shown. $\sigma(\Delta\nu^{A',170})$, $\sigma(A)$, and $\sigma(B)$ indicated in parenthesis represents the total uncertainties [9].

$\Delta\nu^{A',170}$ (MHz)			^{167}Er HFS coefficients				
$4f^{12}6s^2\ ^3H_6 \rightarrow 4f^{12}(^3H)6s6p\ J = 5$			$4f^{12}6s^2\ ^3H_6$			$4f^{12}(^3H_5)6s6p\ J = 5$	
Mass number	gas jet	ABU [9]	Method	A (MHz)	B (MHz)	A (MHz)	B (MHz)
168	96(6)	97(8)	gas jet	−122(3)	−4847(237)	−148(4)	−2230(200)
167	138(8)	132(10)	gas jet	−121.8(fixed)	−4563(fixed)	−147.1(7)	−1936(24)
166	196(7)	193(8)	ABU [9]	−121.80(75)	−4563(53)	−147.66(83)	−1888(58)
164	283(7)	298(7)	[31,32]	−120.487(1)	−4552.984(10)	−146.6(3)	−1874(16)

based on [12,16] were performed. For the calculated values, a weighted average of the centroid and FWHM values from the SATLAS fits were considered for the ^{170}Er resonance. The transverse first-step laser configuration was used to determine the atomic transition frequency (ν_{01}) of the ^{170}Er atom ν_{01} = 721,995,054(60) MHz. The local temperature of the gas jet was determined from the Doppler FWHM and atomic transition frequency. The Doppler FWHM was calculated from the FWHM of the ^{170}Er resonance after subtracting the contribution of the natural and laser linewidths. The resulting value was 268(5) MHz from which the local temperature of the jet was deduced to be 46(2) K. The atoms flushed out with the buffer gas in the jet are assumed to have the same velocity and temperature as that of the buffer gas atoms. The counter-propagating first-step laser configuration was used to measure the Doppler shifted centroid of the ^{170}Er resonance ν_{02} = 721,993,693(60) MHz from which the stream velocity of the jet u = 565(35) m/s was calculated. The Mach number was calculated to be M = 4.5(3) from the stream velocity (u) and speed of sound (a) derived from the temperature of the gas jet. The deduced temperature in the gas cell is T_0 = 353(16) K for the deduced Mach number. The deduced Mach number is lower than the value reported in [16] which might be due to a possible misalignment in the laser path or inhomogeneity of the jet.

4. Conclusion and outlook

The first off-line laser ionization and spectroscopy tests were carried out with the S^3-LEB setup. These results show the potential of the setup to perform high-resolution laser spectroscopy for on-line studies. These results show an order of magnitude better resolution than those in conventional gas cell experiments, as seen for Er, which at this stage of development, gives encouraging prospects for laser spectroscopy of heavy elements. The in-gas-cell and in-gas-jet resonance laser ionization were explored in detail and the transmission across the whole setup until the MR-TOF-MS was optimized to obtain a preliminary transmission efficiency of 20% from the gas jet to the end of PILGRIM, assuming an efficiency close to 100% for the S-RFQ and m-RFQ. This overall efficiency includes the ion bunching efficiency and the subsequent transmission to PILGRIM. The transmission from the cooler-buncher to PILGRIM is currently 50%. In the future, the connecting part to PILGRIM will be replaced by a 90° bender to couple to SEASON. The foreseen re-alignment of the ion cooler-buncher unit gives room for improvement of the transmission efficiency. The collisional effects in the gas cell ionization were quantified for the transition used to study Er isotopes. The isotope shift and the hyperfine constants were measured and they are in good agreement with the literature values [9, 30–32]. The determined Mach number of the jet is below expectation requiring more systematic studies of the jet conditions which will be performed in the future together with a relative measurement of the laser ionization efficiency in the gas cell and the gas jet. With these off-line measurements, the setup is validated for future on-line experimental studies at S^3.

Declaration of competing interest

The authors declare that they have no known competing financial interests or personal relationships that could have appeared to influence the work reported in this paper.

Acknowledgments

S^3 has been funded by the French Research Ministry, National Research Agency (ANR), through the EQUIPEX (EQUIPment of

EXcellence) reference ANR-10EQPX-46, the FEDER (Fonds Europeen de Developpement Economique et Regional), under contract No. FEDER 0111251-21E03702, the CPER (Contrat Plan Etat Région), under contract No. 15P04209 and supported by the U.S. Department of Energy, Office of Nuclear Physics, under contract No. DE-AC02-06CH11357 and by the E.C.FP7 INFRASTRUCTURES 2007, SPIRAL2 Preparatory Phase, Grant agreement No. 212692. S^3-LEB has received funding from the French Research Ministry through the ANR-13-BS05-0013, the Research Foundation Flanders (FWO) under the International Research Infrastructure program (nr. I002219N), the FWO and F.R.S.-FNRS EOS program (nr. 40007501), the Research Coordination Office KU Leuven, the European Research Council (ERC-2011-AdG-291561-HELIOS), the European Union's Horizon 2020 research and innovation program under grant agreement No 654002 and No 861198–LISA–H2020-MSCA-ITN-2019, and the IN2P3-GSI collaboration under agreement No PN1064.

References

[1] S. Gales, SPIRAL2 at GANIL: next generation of ISOL facility for intense secondary radioactive ion beams, Nuclear Phys. A 834 (1–4) (2010) 717–723.
[2] A. Orduz, P.-E. Bernaudin, M. Di Giacomo, R. Ferdinand, B. Jacquot, O. Kamalou, J.-M. Lagniel, G. Normand, A. Savalle, D. Uriot, SPIRAL2 final commissioning results, in: 31st Linear Accelerator Conference, 2022, TU2AA02.
[3] F. Dechery, H. Savajols, M. Authier, A. Drouart, J. Nolen, D. Ackermann, A. Amthor, B. Bastin, A. Berryhill, D. Boutin, et al., The Super Separator Spectrometer S^3 and the associated detection systems: SIRIUS and LEB-REGLIS^3, Nucl. Instrum. Meth. B 376 (2016) 125–130.
[4] F. Dechery, A. Drouart, H. Savajols, J. Nolen, M. Authier, A. Amthor, D. Boutin, O. Delferriére, B. Gall, et al., Toward the drip lines and the superheavy island of stability with the Super Separator Spectrometer S^3, Eur. Phys. J. A 51 (2015) 1–16.
[5] R. Ferrer, B. Bastin, D. Boilley, P. Creemers, P. Delahaye, E. Liénard, X. Fléchard, S. Franchoo, L. Ghys, M. Huyse, et al., In gas laser ionization and spectroscopy experiments at the Superconducting Separator Spectrometer (S^3): Conceptual studies and preliminary design, Nucl. Instrum. Meth. B 317 (2013) 570–581.
[6] Y. Kudryavtsev, P. Creemers, R. Ferrer, C. Granados, L. Gaffney, M. Huyse, E. Mogilevskiy, S. Raeder, S. Sels, P. Van Den Bergh, et al., A new in-gas-laser ionization and spectroscopy laboratory for off-line studies at KU Leuven, Nucl. Instrum. Meth. B 376 (2016) 345–352.
[7] P. Chauveau, P. Delahaye, G. De France, S. El Abir, J. Lory, Y. Merrer, M. Rosenbusch, L. Schweikhard, R. Wolf, PILGRIM, a multi-reflection time-of-flight mass spectrometer for SPIRAL2-S^3 at GANIL, Nucl. Instrum. Meth. B 376 (2016) 211–215.
[8] J. Romans, A. Ajayakumar, M. Authier, F. Boumard, L. Caceres, J.-F. Cam, A. Claessens, S. Damoy, P. Delahaye, P. Desrues, et al., First offline results from the S^3 low-energy branch, Atoms 10 (1) (2022) 21.
[9] J. Romans, A. Ajayakumar, M. Authier, F. Boumard, L. Caceres, J.-F. Cam, A. Claessens, S. Damoy, P. Delahaye, P. Desrues, et al., High-resolution laser system for the S^3-Low Energy Branch, Nucl. Instrum. Meth. B 536 (2023) 72–81.
[10] S. Raeder, M. Dombsky, H. Heggen, J. Lassen, T. Quenzel, M. Sjödin, A. Teigelhöfer, K. Wendt, In-source laser spectroscopy developments at TRILIS—towards spectroscopy on actinium and scandium, Hyperfine Interact. 216 (1) (2013) 33–39.
[11] B. Marsh, B. Andel, A. Andreyev, S. Antalic, D. Atanasov, A. Barzakh, B. Bastin, C. Borgmann, L. Capponi, T.E. Cocolios, et al., New developments of the in-source spectroscopy method at RILIS/ISOLDE, Nucl. Instrum. Meth. B 317 (2013) 550–556.
[12] Y. Kudryavtsev, R. Ferrer, M. Huyse, P. Van den Bergh, P. Van Duppen, The in-gas-jet laser ion source: Resonance ionization spectroscopy of radioactive atoms in supersonic gas jets, Nucl. Instrum. Meth. B 297 (2013) 7–22.
[13] R. Ferrer, A. Barzakh, B. Bastin, R. Beerwerth, M. Block, P. Creemers, H. Grawe, R. de Groote, P. Delahaye, X. Fléchard, et al., Towards high-resolution laser ionization spectroscopy of the heaviest elements in supersonic gas jet expansion, Nature Commun. 8 (1) (2017) 1–9.
[14] M. Vandebrouck, Spectroscopy Electron Alpha in Silicon bOx couNter – SEASON, https://anr.fr/Project-ANR-20-CE31-0005.
[15] R. Ferrer, M. Verlinde, E. Verstraelen, A. Claessens, M. Huyse, S. Kraemer, Y. Kudryavtsev, J. Romans, P. Van den Bergh, P. Van Duppen, et al., Hypersonic nozzle for laser-spectroscopy studies at 17 K characterized by resonance-ionization-spectroscopy-based flow mapping, Phys. Rev. Res. 3 (4) (2021) 043041.
[16] A. Zadvornaya, P. Creemers, K. Dockx, R. Ferrer, L. Gaffney, W. Gins, C. Granados, M. Huyse, Y. Kudryavtsev, M. Laatiaoui, et al., Characterization of supersonic gas jets for high-resolution laser ionization spectroscopy of heavy elements, Phys. Rev. X 8 (4) (2018) 041008.
[17] C. Mattolat, S. Rothe, F. Schwellnus, T. Gottwald, S. Raeder, K. Wendt, An all-solid-state high repetiton rate titanium: Sapphire laser system for resonance ionization laser ion sources, in: AIP Conference Proceedings, Vol. 1104, No. 1, American Institute of Physics, 2009, pp. 114–119.
[18] S. Rothe, V. Fedosseev, T. Kron, B. Marsh, R. Rossel, K. Wendt, Narrow linewidth operation of the RILIS titanium: Sapphire laser at ISOLDE/CERN, Nucl. Instrum. Meth. B 317 (2013) 561–564.
[19] V. Sonnenschein, I. Moore, S. Raeder, M. Reponen, H. Tomita, K. Wendt, Characterization of a pulsed injection-locked Ti: sapphire laser and its application to high resolution resonance ionization spectroscopy of copper, Laser Phys. 27 (8) (2017) 085701.
[20] N. Lecesne, R. Alvès-Condé, E. Coterreau, F. De Oliveira, M. Dubois, J. Flambard, H. Franberg, T. Gottwald, P. Jardin, J. Lassen, et al., GISELE: A resonant ionization laser ion source for the production of radioactive ions at GANIL, Rev. Sci. Instrum. 81 (2) (2010) 02A910.
[21] D. Etasse, Introduction to the FASTER Acquisition System, Tech. Rep., http://faster.in2p3.fr/index.php/about-faster.
[22] D. Studer, Resonanzionisationsspektroskopie hochliegender Zustände in Dysprosium und Erbium zur Entwicklung effizienter Anregungsschemata und Bestimmung des ersten Ionisationspotentials (Diploma thesis), Johannes Gutenberg-Universität Mainz, 2015.
[23] Y. Balasmeh, The PILGRIM Mass Spectrometer: Toward High Accuracy Measurements of Exotic Nuclei at S^3 (Master's thesis), Normandie Université, 2022.
[24] B.M. Retailleau, PILGRIM: un spectromètre de masse par temps de vol pour S^3, et brisure de symétrie d'isopin dans le 38K (Ph.D. thesis), Normandie Université, 2021.
[25] N. Allard, J. Kielkopf, The effect of neutral nonresonant collisions on atomic spectral lines, Rev. Modern Phys. 54 (4) (1982) 1103.
[26] G.W. Drake, Springer Handbook of Atomic, Molecular, and Optical Physics, Springer Science & Business Media, 2006.
[27] A. Raggio, I. Pohjalainen, I.D. Moore, Observation of collisional de-excitation phenomena in plutonium, Atoms 10 (2) (2022) 40.
[28] A. Kramida, Y. Ralchenko, J. Reader, NIST ASD Team, NIST Atomic Spectra Database (version 5.10), [Online] Available: https://physics.nist.gov/asd [Mon Apr 03 2023], National Institute of Standards and Technology, Gaithersburg, MD 2023.
[29] W. Gins, R.P. de Groote, M.L. Bissell, C.G. Buitrago, R. Ferrer, K.M. Lynch, G. Neyens, S. Sels, Analysis of counting data: Development of the SATLAS Python package, Comput. Phys. Comm. 222 (2018) 286–294.
[30] H. Okamura, S. Matsuki, Isotope shift in erbium I by laser-atomic-beam spectroscopy, Phys. Rev. C 35 (4) (1987) 1574.
[31] W.J. Childs, L.S. Goodman, V. Pfeufer, Hyperfine structure of the $4f^{12}\ 6s^2\ ^3$H and ^{3}F terms of ^{167}Er I by atomic-beam, laser-rf double resonance, Phys. Rev. A 28 (1983) 3402–3408.
[32] S. Ahmad, C. Ekstrom, W. Klempt, R. Neugart, K. Wendt, Nuclear spins and moments of radioactive odd-A isotopes of erbium studied by collinear fast-beam laser spectroscopy, in: Proceedings of the "Symposium on Quantum Electronics", 1985.